

EVALUATING THE INTRINSIC PERMEABILITY USING A FALLING HEAD GAS PERMEAMETER

Chiara Villani, Kenneth A. Snyder and W. Jason Weiss

Abstract

This paper examines the pressure-dependent gas permeability in cementitious systems, as measured using a falling head gas permeameter. A series of experiments were performed on mortars with varying mixture proportions, and measurements were made with different initial applied pressures. The governing equation is based on an analogy to a falling head liquid permeameter, but accounting for the gas compressibility and the pressure-dependent Klinkenberg effect that can occur during gas permeation. This formulation overcomes a limitation of other approaches that depend on the initial pressure that is applied and on the range of data that can be considered when evaluating transport properties. Analyses of the experimental data confirm that the apparent permeability is inversely proportional to the pressure applied via the Klinkenberg equation. By accounting for this effect, it is possible to determine an intrinsic permeability that is independent of the pressure, and is a true characteristic of the pore space available for gas transport.

Keywords

Gas transport, intrinsic permeability, concrete

1. Introduction

The scientific community is interested in determining the gas transport properties of cementitious materials for potential use in service life prediction (Basheer et al., 2001, Torrent and Luco, 2007, Yuan and Santhanam, 2013). Gas transport testing may be more desirable than liquid transport testing due to the shorter time frame that is required to perform the gas transport measurement and due to the quasi-nondestructive nature of the test (Villani et al., 2014a). However, designing a gas transport test for concrete that is sensitive, robust, easy to perform, and that measures a true material property is challenging for concrete. Gas transport through concrete has been shown to depend on the pressure applied (Abbas et al., 1999) and on the gas flow rate (Lawrence, 1984). Sample conditioning is another critical factor because gas permeability depends on the degree of saturation (Abbas et al., 1999, Houst and Wittmann, 1994, Parrott and Hong, 1991, Villani et al., 2014a, Villani et al., 2014b) and on the presence of micro-cracks that can form during harsh drying processes (Wong et al., 2009). One challenge in developing a permeability test is using the appropriate confining pressure to prevent flow along the outside surface of the specimen without changing the microstructure of the sample. Wu et al. (2013) reported the dependence of oxygen diffusion measurements on the confining pressure applied to concrete samples to ensure one-dimensional flow. The authors argued that the confinement could cause the closure of micro-cracks and consequently a reduction in gas transport would be expected (Wu et al., 2013). Additionally, gas transport can be altered by reaction mechanisms like carbonation or further hydration (Houst and Wittmann, 1994, Villani et al., 2014a).

This paper investigates the influence of pressure on the gas permeability that is measured using a falling head gas permeameter. The setup consists of a fixed-volume gas chamber connected, via a shut-off valve, to one end of a cylindrical specimen, and the opposite end of the specimen exhausts to the laboratory. A measurement consists of pressurizing the fixed-volume chamber to a

predetermined pressure, opening the valve, and then recording the drop in pressure over time as the gas is transported through the specimen. The experimental apparatus and testing conditions are based on the approach proposed by Alexander et al. (2007). The current study, however, uses a new approach to analyze the test data so that one may determine the intrinsic permeability of the concrete (i.e., a material property that is independent of the fluid or the fluid pressure).

2. Experimental Details

2.1 Materials

The samples used in this study were mortars with water-to-cement ratio by mass (w/c) of 0.30, 0.40, 0.42 and 0.50, and a constant fine aggregate volume of 55 % of the total volume. The fine aggregates were a natural river sand with a fineness modulus of 2.70 and a maximum aggregate size of 4.75 mm. The mixture proportions are summarized in Table 1. The mixing procedure was performed in accordance with (ASTM C192-12a).

Table 1: Compositions of the mortar mixtures. Mixture M30 was made using a water-reducing admixture (WRA).

	M30	M40	M42	M50
Type I portland cement [kg/m ³]	706.8	610.0	595.1	535.6
Fine Aggregates [kg/m ³]	1389.0	1382.3	1382.0	1380.7
Water [kg/m ³]	237.3	270.6	275.4	294.8
WRA [kg/m ³]	4.3	-	-	-
w/c	0.30	0.40	0.42	0.50

Cylindrical samples (approximately 102 mm diameter, and 204 mm long) were prepared for each

mixture. The mortar cylinders were consolidated using external vibration. After consolidation, the samples were sealed with lids immediately after casting, and stored in an environmental chamber at $(23 \pm 2) ^\circ\text{C}$. The cylinders were demolded at an age of 24 h, placed in double-layered, re-sealable plastic bags, and returned to the environmental chamber for 28 d. At an age of 28 d the cylinders were cored along the central axis of the cylinder. The cores were then cut to length, from the middle portion of the core, using a wet saw. The final specimens had a (68 ± 2) mm (2.7 in.) diameter and a (30 ± 2) mm (1.2 in.) length (Villani et al., 2014b); uncertainties represent the measured standard deviation from repeated measurements on multiple specimens.

Each specimen belonging to mixtures M30, M40 and M50 was oven dried at $(50 \pm 0.5) ^\circ\text{C}$ in a convection oven for 7 d, or until its mass was stable (a mass change less than 0.1 % for three consecutive days). Prior to the test, each specimen was brought to room temperature in a closed vessel for 2 h at $(23 \pm 1) ^\circ\text{C}$. Although the permeability obtained from samples that are oven dried might be considerably different from the permeability measured on concrete belonging to a structure in the field, this study focuses on the methodology used for the evaluation of permeability.

Samples belonging to mixture M42 were tested after being conditioned for 18 months at a temperature of $(23 \pm 0.5) ^\circ\text{C}$ and in relative humidity (RH) controlled chambers with one set of samples at $(65 \pm 1) \% \text{RH}$ and another set at $(50 \pm 2) \% \text{RH}$.

To investigate the influence of pressure on the gas permeability, four specimens from each of the four mixtures (M30, M40, M42 and M50) were tested at three different initial absolute pressures (151 kPa, 201 kPa and 251 kPa). The initial absolute pressure recommended by Alexander et al. (2007) was 201 kPa. For all the measurements, the atmospheric pressure of the laboratory was

assumed to be 101 kPa.

2.2 Testing Method

Oxygen permeability was measured using a falling head gas permeameter commonly known as the South African permeameter following the procedure recommended by Ballim (Ballim, 1991, Alexander, 2007). The South African permeameter uses a cylindrical sample that is inserted in a rubber collar (to ensure one-dimensional gas flow) and exposed to a pressure gradient. One end of the specimen is in contact with a vessel that is initially pressurized to a known oxygen pressure, and the other end is exposed to atmospheric pressure. Once the valve between the specimen and the vessel is opened, the oxygen permeability can be estimated from the recorded pressure decay over time in the oxygen vessel. More details about the test procedure can be found in Alexander et al. (Alexander, 2007, Villani et al., 2014a).

3. Results

The results obtained from the oxygen permeability measurements are presented hereafter in a comparison between the current calculation approach (Ballim, 1991, Alexander et al., 1999) and an approach based on the derivation described in this paper. For each approach, the formulation is also provided.

3.1 Existing oxygen permeability formulation

The oxygen permeability formulation originally proposed for the South African permeameter (Ballim, 1991) was developed using a combination of Darcy's law and the ideal gas law. The resulting equation for the apparent permeability (k_{SA}) is shown below in Equation (1):

$$k_{SA} = \frac{M V_v L g}{R T \Delta t A} \ln \frac{P_i}{P} \quad (1)$$

where M is the molecular mass of oxygen (0.032 kg/mol), V_v is the volume of the oxygen vessel, L is the sample length, g is the gravitational acceleration, R is the universal gas constant (8.314 N m/(K mol)), T is the thermodynamic temperature, A is the sample cross sectional area, P_i is the initial vessel pressure, and P is the pressure in the vessel after a time interval Δt . It should be noted that Equation (1) is derived under the assumption that the coefficient of permeability does not depend on either pressure or time (Ballim, 1991, Villani, 2014). Under this assumption, Equation (1) indicates that it will take the same time interval Δt for the pressure in the vessel to fall to the same fraction of the initial pressure, regardless of the initial pressure.

Figure 1 provides typical results of the tests performed on oven dry samples. Figure 1 shows the coefficient of permeability (k_{SA}) as function of the inverse of the average initial pressure P_m (the average of the initial vessel pressure P_i and the atmospheric pressure P_o). In Figure 1 the coefficient of permeability has been evaluated according to the procedure described in Ballim (1991) (Equation (1)). The test was performed considering two approaches. The first approach used data from 6 hours of testing (solid symbols) and the second approach used only the data interval gathered over the time when the pressure had dropped from its original value to half of its initial value (hollow symbols). The two data sets are analyzed using the prescribed approach ((Alexander, 2007, Ballim, 1991)). The error bars reported in Figure 1 indicate the standard deviation obtained from the four samples tested in the same conditions (i.e., initial applied pressure) and using the

same calculation approach (6 hours testing data or data gathered over the time interval Δt the pressure dropped to one-half of initial value).

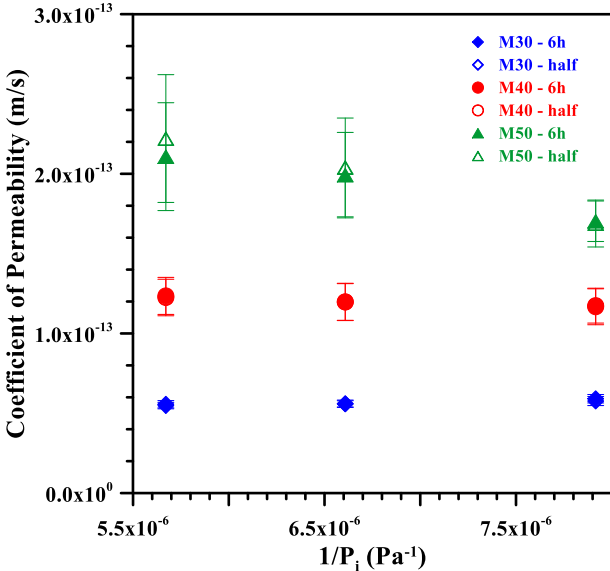


Figure 1: The coefficient of oxygen permeability (k_{SA}) as a function of the initial average pressure P_m , for mortar mixtures with varying w/c and dried at 50 °C. Uncertainty represents the standard deviation from 4 specimens.

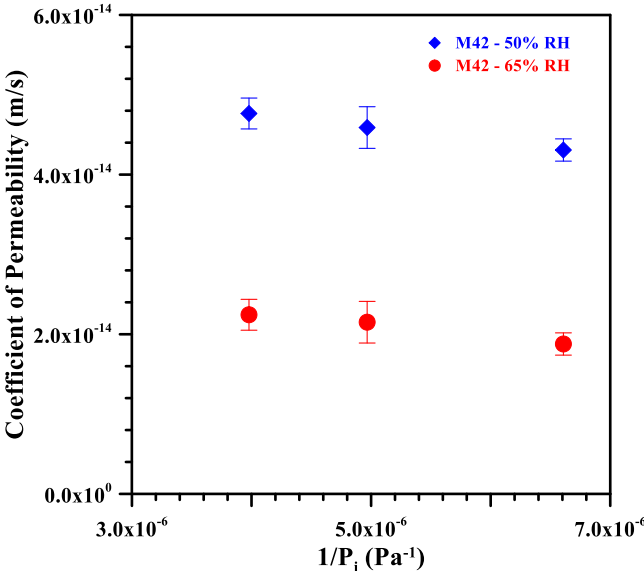


Figure 2: The coefficient of oxygen permeability (k_{SA}) as a function of the initial average pressure

P_m , for the M42 mortar mixtures dried to 50 % RH and 65 % RH. Uncertainty represents the standard deviation from 4 specimens.

The coefficients of permeability plotted in Figure 1 show a pressure dependence over the testing time interval considered (both the 6 hours testing data and the data corresponding to a pressure drop equal to half of the initial relative pressure value). The variability in the measured permeability, due to the variation in the interval of data that is used, ranged between 0.1 % and 5 %. The greater variations were observed for higher permeability samples ($w/c = 0.50$). Figure 1 also indicates that the measured permeability depends on the initial vessel pressure used in the measurement (Villani et al., 2014a). An increase in permeability occurred when a higher initial pressures was used for M50 mix. This is opposite to the expected response. Researchers (Abbas et al., 1999, Kropp et al., 2007) have used porous samples to demonstrate a decrease in gas permeability at higher pressure due to the “slip” effect at the pores walls and have described this as the *Klinkenberg effect* (Klinkenberg, 1941). The same unexpected pressure dependence as a function of the applied pressure is also seen in Figure 2, where the measured coefficient of permeability (Ballim, 1991) of mixtures M42 conditioned to 50% RH and to 65%RH is greater when a higher initial pressure is applied.

Based on this unexpected behavior that arises when performing an analysis based on the South African equation, an alternative formulation was developed and is described in the following section.

3.2 Proposed oxygen permeability formulation

The equation describing the flow of oxygen in the falling head gas permeameter can be derived

using an analogy to a falling head liquid permeameter. For the liquid permeameter, the liquid is assumed to be incompressible. As a result, at steady-state the mass flow rate and the volumetric flow rate are both constant. For a gas permeameter at steady-state, only the mass flow rate is constant. To relate the mass flow rate to the volumetric flow rate, one uses an equation of state for the fluid, assumed here to be the ideal gas law:

$$PV = \frac{m}{M}RT = \omega \quad (2)$$

where P is the gas pressure when occupying a volume V , m is the mass of the gas in volume V , and ω is the *reduced* mass. (This quantity has been introduced here for purely algebraic convenience.) Based on this relationship, the *reduced* gas density (ω/V) is equal to the pressure P , and the volumetric flow rate \dot{q} is related to the reduced mass flow rate $\dot{\omega}$ via the pressure: $\dot{\omega} = P\dot{q}$, assuming isothermal conditions, which is consistent with throttling an ideal gas (Reidi 1988). With this relationship, one can now relate the mass flow rate to the volumetric flow rate of an ideal gas.

The flow of a fluid through a porous material is characterized by the Darcy equation:

$$\mathbf{v}_D = \frac{-k}{\mu} \nabla P \quad (3)$$

where \mathbf{v}_D is the Darcy velocity, k is the permeability and μ is the fluid viscosity. The volumetric flow rate is related to the Darcy velocity of a fluid passing through an area A having a surface unit normal in direction \hat{z} :

$$\dot{q} = A\hat{z} \cdot \mathbf{v}_D = \frac{-kA}{\mu} \hat{z} \cdot \nabla P \quad (4)$$

Subsequent analysis will assume that the fluid flow is one-dimensional, is perpendicular to the area A , and is parallel to the normal vector in direction \hat{z} . Furthermore, the falling head fluid permeameter is analyzed under the assumption that, although the inlet pressure is slowly decreasing, the rate of change is small enough that the device operates in a *quasi* steady-state condition. Therefore, it is assumed that because the pressure of the upper vessel changes very slowly, the *reduced* mass flow rate $\dot{\omega}$ is a constant throughout the specimen at any given moment:

$$\dot{\omega} = P\dot{q} = \frac{kA}{\mu} P\nabla P = \frac{kA}{2\mu} \frac{\partial P^2}{\partial z} \quad (5)$$

Because this quantity is a constant, the right hand side can be written algebraically by evaluation the right-hand expression at the boundaries:

$$\dot{\omega} = \frac{kA}{2\mu L} (P_v^2 - P_o^2) \quad (6)$$

where L is the thickness of the specimen, P_v^2 is the upper vessel pressure, and P_o^2 is the outlet pressure (for the oxygen permeameter analyzed in this study P_o is equal to the atmospheric pressure). The *reduced* mass flow rate $\dot{\omega}$ is related to the change in the pressure of the upper vessel via Eq. (2) (the vessel volume is a constant), which would then be equal to the *reduced* flow rate in Eq. 7:

$$\dot{\omega} = V_v \frac{\partial P_v}{\partial t} = \frac{kA}{2\mu L} (P_v^2 - P_o^2) \quad (7)$$

where V_v is the volume of the upper vessel. Assuming that the permeability and the viscosity do not depend upon pressure (or are very weak functions of pressure), the equation is separable:

$$\int_{P_i}^P \frac{dP_v}{(P_v^2 - P_o^2)} = \frac{-kA}{2\mu LV_v} \int_{t_o}^{t_o+\Delta t} dt \quad (8)$$

where P_i is the initial vessel pressure at time t_o , and Δt is the duration of time required for the pressure to fall from P_i to P . The solution to this equation gives the following expression for the time-dependent pressure of the upper vessel (Gradshteyn et al., 1965, Villani, 2014):

$$P = P_o \coth \left(\frac{k AP_o}{2 \mu L V_v} (\Delta t) + \coth^{-1} \left(\frac{P_i}{P_o} \right) \right) \quad (9)$$

It has been shown that the apparent gas permeability of porous materials depend upon the pressure at which the measurement was performed (Abbas et al., 1999). This pressure dependence has been characterized by the Klinkenberg (Klinkenberg, 1941) equation relating the apparent permeability k_a to the intrinsic material permeability k_{in} , via the Klinkenberg parameter b :

$$k_a = k_{in} \left(1 + \frac{b}{P} \right) \quad (10)$$

This equation differs from typical applications of the Klinkenberg equation in that Eq. (10) is a function of the time-dependent boundary (vessel) pressure, not the average pressure across the specimen. This distinction is important because the Klinkenberg equation is most often applied to data from a steady-state experiment, for which the average pressure has a well-defined meaning. Here, a quasi-steady state is assumed, so the falling-head permeameter can be thought of as a sequence of steady-state measurements. As the Klinkenberg parameter b should be independent of the boundary conditions, the same should be true for the falling head permeameter. As written, however, the precise value of the parameter b would differ from an analysis from a steady-state measurement and using the average pressure.

The pressure dependence in Eq. (10) could be incorporated into the analysis in one of two ways. The first way is to repeat the integral in Eq. (8) by replacing the permeability k with the apparent permeability k_a in Eq. (10), and solving the (more complicated) integral; the resulting equation is rather complex, obfuscating a physical interpretation. The second way is to assume that because the pressure dependence is a very weak function of pressure, the apparent permeability in Eq. (10) can be inserted directly into the result in Eq. (9). This second method (inserting the apparent permeability of Eq. (10) directly in Eq. (9)) was used by (Wu et al., 1998) for evaluating materials having relatively small values of the ratio b/P . The resulting expression (Eq. (11)) is similar to the equation obtained by Gardner et al. (2008) for studying the Klinkenberg effect in a nitrogen falling head permeameter using radial gas flow through a cylindrical annulus of concrete (Gardner et al., 2008):

$$P = P_0 \coth \left(k_{in} \left(1 + \frac{b}{P} \right) \cdot \chi \cdot t + \tau \right) \quad (11)$$

For the one-dimensional gas flow used here, χ and τ are constants as defined below in Equation (12) and Equation (13):

$$\chi = \frac{AP_0}{2 \mu L V_v} \quad (12)$$

$$\tau = \coth^{-1} \left(\frac{P_i}{P_0} \right) \quad (13)$$

There are a number of approaches for analyzing experimental data using Equation (11). In the work by Gardner et al., the Klinkenberg parameters (k_{in} and b) were found using only two data points of known pressure (P_1 and P_2) and time (t_1 and t_2) recorded during the pressure decay. Specifically, Gardner et al. suggested using the pressure data and time corresponding to a pressure

drop of $\frac{1}{2}$ the original value ($P_{1/2}$ and $t_{1/2}$) and $\frac{3}{4}$ of the original value ($P_{3/4}$ and $t_{3/4}$). This approach has been applied to the data obtained from the falling head gas permeameter used in this study, and it has been observed that the calculated parameters (k_{in} and b) depend on the pressure data used in the analysis. Specifically, depending on the pressure (P_1 and P_2) and time (t_1 and t_2) data selected for the calculation, the intrinsic permeability changes by approximately 20 %, and the Klinkenberg parameter changes by up to 90 % (Villani, 2014).

The alternative approach that is suggested here uses all the pressure decay data (pressure and time) obtained from the test to evaluate the intrinsic permeability and the Klinkenberg parameter. Equation (11) is rearranged to isolate the apparent permeability (Equation (10)) in Equation (14) (Klinkenberg, 1941):

$$k_a(P) = \frac{\tanh^{-1}\left(\frac{P_0}{P}\right) - \tanh^{-1}\left(\frac{P_0}{P_i}\right)}{\chi t} = k_{in} \left(1 + \frac{b}{P}\right) \quad (14)$$

The middle term of Equation 14 contains the measureable quantities (P and t), and the value of this quantity should vary linearly when plotted against the inverse of pressure. When applying linear regression upon the data, the y-intercept of the line will be an estimate of the intrinsic permeability k_{in} , and the slope will be an estimate of the product ($k_{in} b$). The linear relationship between the apparent permeability and the inverse of vessel pressure is plotted in Figure 3 for a typical specimen that was oven-dried from mixture M40, and tested using three different initial pressures.

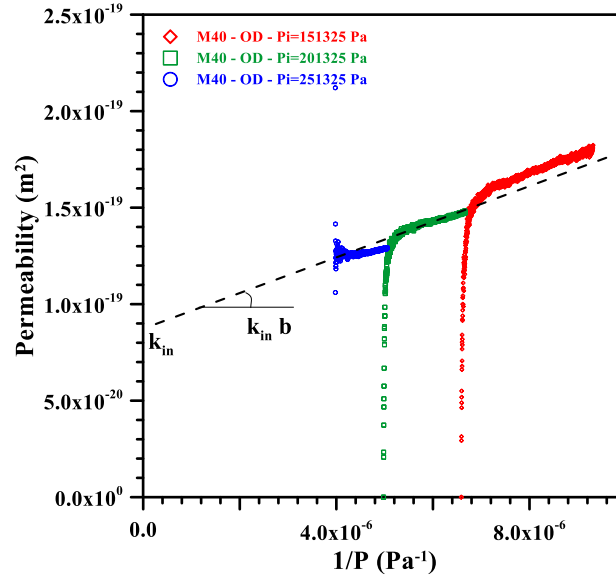


Figure 3: Plot of the apparent permeability as a function of the inverse pressure vessel pressure P , confirming the linear relationship expected from Klinkenberg equation (Klinkenberg, 1941)

When analyzed in this manner, the data show an initial transient that results from establishing the steady-state pressure gradient across the sample immediately after the valve is opened. After the mass flow rate has become a constant throughout the specimen, the data exhibit the expected linear dependence on the inverse of the vessel pressure. The initial non-linear portion of pressure/time data has been excluded in the evaluation of the intrinsic permeability.

The experimental data have also been used to confirm the reduction in the slope ($k_{in} \cdot b$) of the Klinkenberg equation with the increase of the conditioning relative humidity (or degree of saturation) as previously noticed by Abbas et al. (1999). The reduction in slope due to the increase of the conditioning relative humidity is shown in Figure 4(a) and Figure 4(b) where the change in permeability with respect to the inverse of pressure in the vessel is shown for, respectively, a

sample in oven dry condition (Figure 4(a)) and a sample conditioned at 50% RH (Figure 4(b)). Both samples belong to mixture M40 and were tested using 201 kPa as the initial pressure.

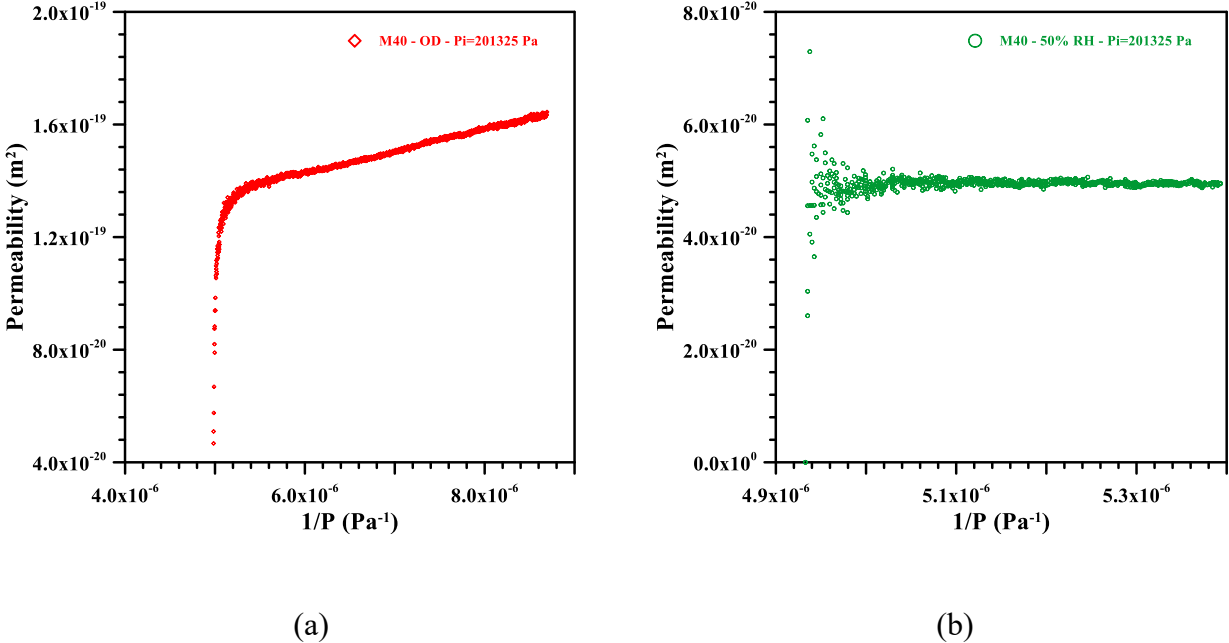


Figure 4: Pressure dependent apparent permeability for an M40 mixture that was (a) oven-dried, and (b) conditioned to 50% RH; both specimens were tested at an initial pressure of 201 kPa.

The linear portion of the experimental data has been fit to Equation (14) and the parameters b and k_{in} were determined by regression analysis. Using these parameters, Equation (11) can be used to predict the measured pressure decay from the experimental data. Figure 5 shows the data for sample #1 conditioned at 50 % RH and tested at three initial pressures. As can be seen in the figure, Equation (11) provides an accurate description of the time-dependent pressure decay in the falling-head gas permeameter.

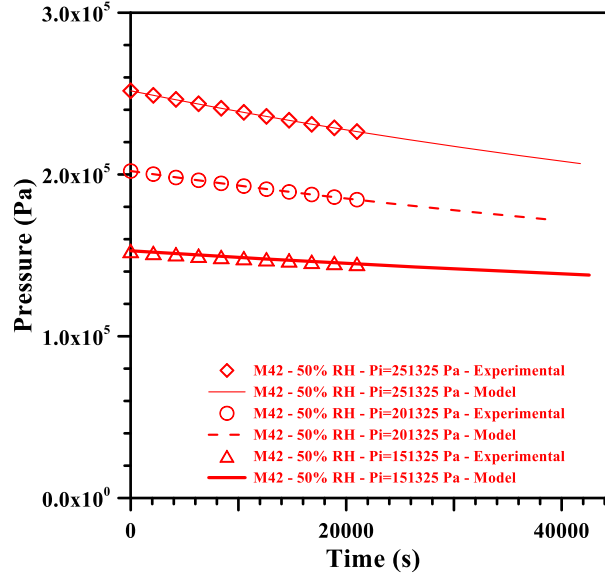


Figure 5: Comparison between predicted (solid line - Equation (14)) and experimental data (open symbols) for mix M42 sample #1 conditioned at 50% RH and tested at three initial pressures (151325 Pa, 201325 Pa and 251325 Pa)

The parameters obtained from the regressions (k_{in} and b) of all the samples tested are listed in Table 2 and Table 3. The reported values are the average and the uncertainty (one standard deviation) was calculated from the four samples tested for each mixture or conditioning RH.

Table 2: Intrinsic permeability and Klinkenberg parameter for oven-dry samples. Uncertainty represents one standard deviation.

	P_i (kPa)	k_{in} (10^{-20} m^2)	b (kPa)
M30	151.3	4.32 ± 1.12	36.1 ± 28.0
	201.3	3.59 ± 0.54	115.4 ± 34.6
	251.3	3.74 ± 0.33	77.3 ± 12.1
M40	151.3	9.67 ± 1.78	79.8 ± 49.0
	201.3	9.04 ± 0.88	74.91 ± 6.74
	251.3	8.55 ± 0.83	75.05 ± 3.20
M50	151.3	19.3 ± 6.05	54.3 ± 44.6
	201.3	22.1 ± 5.08	0.2 ± 21.2
	251.3	20.0 ± 6.02	13.6 ± 33.1

Table 3: Intrinsic permeability and Klinkenberg parameter for M42 samples conditioned at 50% RH and 65% RH. Uncertainty represents one standard deviation.

	P_i (Pa)	k_{in} (m ²)	k_{in} SD (m ²)	b (Pa)	b SD (Pa)
50% RH	151325	$4.22 \cdot 10^{-20}$	$4.68 \cdot 10^{-21}$	39829	31556
	201325	$4.30 \cdot 10^{-20}$	$3.01 \cdot 10^{-21}$	31747	4447
	251325	$3.93 \cdot 10^{-20}$	$2.48 \cdot 10^{-21}$	38755	17242
65% RH	151325	$2.20 \cdot 10^{-20}$	$6.95 \cdot 10^{-21}$	2280	1498
	201325	$1.91 \cdot 10^{-20}$	$3.68 \cdot 10^{-21}$	25945	33791
	251325	$1.90 \cdot 10^{-20}$	$5.86 \cdot 10^{-21}$	25274	7745

The parameters presented in Table 2 and Table 3 are within the range found in previous work (Abbas et al., 1999, Gardner et al., 2008). The values of the Klinkenberg parameters b for the samples conditioned at 50% RH and 65% RH (Table 3) are generally smaller than the values for the oven-dried specimens, and are generally a factor of ten smaller than the initial vessel pressure. Therefore, the apparent permeability k_a is relatively constant over the range of pressures considered, and is nearly equal to the intrinsic permeability.

An anomalous behavior was seen for some M50 samples tested after oven drying. These specimens show a large variability (large coefficient of variation) in the Klinkenberg parameters (k_{in} and b) as well as a negative b parameter values that result in very a low average b value. This is believed to be due to micro-cracking caused by the oven-drying process that generates a more highly permeable system in the high water to cement ratio samples. This is consistent with other observations on highly permeable concrete specimens where the Klinkenberg effect was found to be negligible (Baroghel-Bouny, 2007).

Figure 6 shows the average intrinsic permeability as function of the inverse of vessel pressure for samples belonging to three mixtures (M30, M40 and M50) and tested after oven-drying. Figure 7

presents the average intrinsic permeability for samples conditioned at 50% RH and 65% RH belonging to M42. It is confirmed that the intrinsic permeability is not a function of the applied pressure. The slight changes seen when the initial pressure is altered (Figure 6 and Figure 7) only reflects the variability of the instrument and of the material (Villani et al., 2014a). The intrinsic permeability results appear to be only a function of the pore space available to gas transport and not the experimental conditions: it varies with changes in the mixture proportions (i.e., water-to-cement ratio) and with change in the conditioning RH (or degree of saturation).

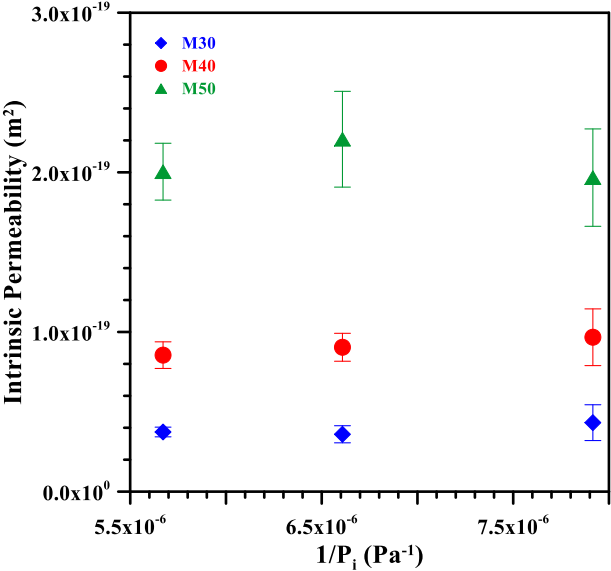


Figure 6: Intrinsic permeability for M30, M40 and M50 samples tested in oven-dry conditions at different initial pressures

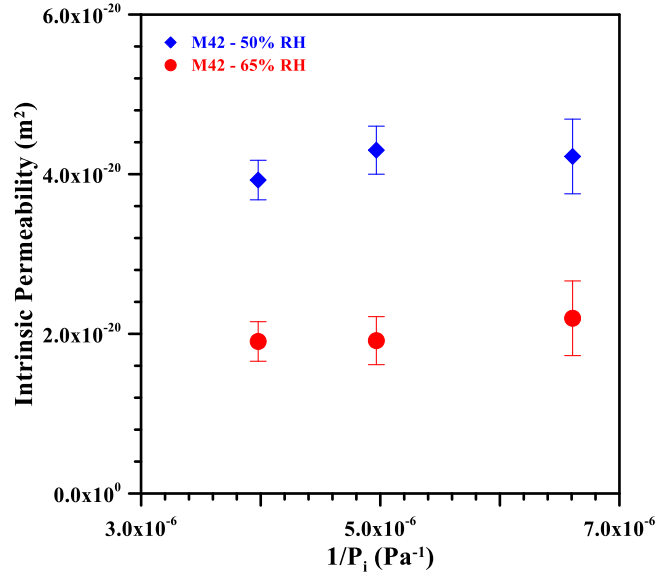


Figure 7: Intrinsic permeability for M42 samples conditioned at 50 % RH and 65 % RH and tested at different initial pressures

4. Summary and Conclusions

This paper presents results from an investigation performed to determine whether varying the initial pressure changes the gas permeability as measured using a falling head gas permeameter. A conventional approach (Ballim, 1991) was used to analyze test data and an alternative approach was developed to consider the dependence of permeability on pressure and the compressibility of the gas in the determination of an intrinsic permeability (i.e., a material property that is independent of pressure). Test data were collected using samples belonging to different mixtures and conditioned using oven drying, 50% RH and 65% RH.

The Ballim approach results in a coefficient of permeability that depends on the initial pressure and the range of data considered (6 hours or until the pressure to half of its initial value) in evaluating the results.

The approach proposed in this paper has been developed combining Darcy's law for compressible fluids and the equation of state for gases, and assuming that the vessel pressure changes slowly enough that the assumption that the mass flow rate is conserved is valid. The resulting equation provides an apparent gas permeability that further allows the evaluation of an intrinsic permeability by relating the apparent permeability to the Klinkenberg expression for the pressure dependence. The experimental data analyzed using this approach confirmed the following:

- the proposed approach can accurately describe the pressure decay of the samples tested in the falling head gas permeameter;
- there is a linear relationship between the apparent permeability and the inverse of the vessel pressure. The slope of this response is function of the mixture proportions and the conditioning relative humidity.
- one can determine an intrinsic permeability that is independent of the applied pressure and that can characterize the pore space available for gas transport.

5. Acknowledgements

This work has been supported in part by the Joint Transportation Research Program administered by the Indiana Department of Transportation in the National Pooled Fund Study titled "Evaluation of Test Methods for Permeability (transport) and Development of Performance Guidelines for Durability" (TPF-5(179)) whose support the authors gratefully acknowledge. The experiments reported in this paper were conducted in the Pankow Materials Laboratories at Purdue University. The authors acknowledge the support that has made this laboratory and its operation possible.

6. References

ABBAS, A., CARCASSES, M. & OLLIVIER, J.-P. 1999. Gas permeability of concrete in relation

- to its degree of saturation. *Materials and Structures*, 32, 3-8.
- ALEXANDER, M. G. 2007. Durability Index Testing Procedure Manual.
- ALEXANDER, M. G., BALLIM, Y. & MACKECHNIE, J. M. 1999. Concrete durability index testing manual. Research Monograph.
- ASTM C192-12A Standard Practice for Making and Curing Concrete Test Specimens in the Laboratory. ASTM International.
- BALLIM, Y. 1991. A low cost falling head permeameter for measuring concrete gas permeability. *Concrete Beton*, 61, 13-18.
- BAROGHEL-BOUNY, V. 2007. Water vapour sorption experiments on hardened cementitious materials: Part I: Essential tool for analysis of hygral behaviour and its relation to pore structure. *Cement and Concrete Research*, 37, 414-437.
- BASHEER, P. M. A., NOLAN, E. & LONG, A. E. 2001. Near surface moisture gradients and in-situ permeation tests. *Construction and Building Materials*, 15, 105-114.
- GARDNER, D. R., JEFFERSON, A. D. & LARK, R. J. 2008. An experimental, numerical and analytical investigation of gas flow characteristics in concrete. *Cement and Concrete Research*, 38, 360-367.
- GRADSHTEYN, I. S., RYZHIK, I. M., JEFFREY, A., ZWILLINGER, D. & TECHNICA, S. 1965. *Table of integrals, series, and products*, Academic press New York.
- HOUST, Y. F. & WITTMANN, F. H. 1994. Influence of porosity and water content on the diffusivity of CO₂ and O₂ through hydrated cement paste. *Cement and Concrete Research*, 24, 1165-1176.
- KLINKENBERG, L. 1941. The permeability of porous media to liquids and gases. *Drilling and Production Practice*. American Petroleum Institute, 200-213.
- KROPP, J., ALEXANDER, M., TORRENT, R. & LUCO, L. F. 2007. Transport mechanisms and reference tests. *Non-Destructive Evaluation of the Penetrability and Thickness of the Concrete Cover-State-of-the-Art Report of RILEM Technical Committee 189-NEC*.
- LAWRENCE, C. D. Transport of oxygen through concrete. In: GLASSER, D. P., ed. *The chemistry and Chemical-related Properties of Cement*, 1984. British Ceramic Society Proceedings, 277-293.
- PARROTT, L. & HONG, C. Z. 1991. Some factors influencing air permeation measurements in cover concrete. *Materials and Structures*, 24, 403-408.
- REIDI, P. C. 1988. *Thermal Physics: An Introduction to Thermodynamics, Statistical Mechanics, and Kinetic Theory* (Second Edition). Oxford University Press, Oxford, England.
- TORRENT, R. & LUCO, L. F. 2007. *Report 40: Non-Destructive Evaluation of the Penetrability and Thickness of the Concrete Cover-State-of-the-Art Report of RILEM Technical Committee 189-NEC*, RILEM publications.
- VILLANI, C. 2014. *Transport Processes in Partially Saturated Concrete: Testing and Liquid Properties* PhD Thesis, Purdue University.
- VILLANI, C., LOSER, R., WEST, M. J., BELLA, C. D., LURA, P. & JASON WEISS, W. 2014a. An inter lab comparison of gas transport testing procedures: oxygen permeability and oxygen diffusivity. *Cement and Concrete Composites*, 53, 357-366.
- VILLANI, C., NANTUNG, T. E. & WEISS, W. J. 2014b. The influence of deicing salt exposure on the gas transport in cementitious materials. *Construction and Building Materials*, 67, 108-114.
- WONG, H. S., ZOBEL, M., BUENFELD, N. R. & ZIMMERMAN, R. W. 2009. Influence of the interfacial transition zone and microcracking on the diffusivity, permeability and sorptivity

- of cement-based materials after drying. *Magazine of Concrete Research*, 61, 571-589.
- WU, Y.-S., PRUESS, K. & PERSOFF, P. 1998. Gas flow in porous media with Klinkenberg effects. *Transport in Porous Media*, 32, 117-137.
- WU, Z., WONG, H. & BUENFELD, N. Effect of confining pressure on gaseous transport properties of concrete. 33rd Cement and concrete science conference, 2013 Portsmouth, UK.
- YUAN, Q. & SANTHANAM, M. 2013. Test Methods for Chloride Transport in Concrete. *Performance of Cement-Based Materials in Aggressive Aqueous Environments*. Springer.